



Agent-based model predictive control of soil–crop irrigation with topographical information

Jorge Lopez-Jimenez^{a,*}, Nicanor Quijano^a, Laurent Dewasme^b, Alain Vande Wouwer^b

^a Department of Electrical and Electronic Engineering, Universidad de los Andes, Cra 1 # 18A - 12, Bogotá, 111711, Colombia

^b Systems, Estimation, Control, and Optimization (SECO), University of Mons, Mons, 7000, Belgium

ARTICLE INFO

Keywords:

Dynamic modeling
Agent-based model
Model predictive control
Irrigation
Water management
Agriculture

ABSTRACT

The amount of water in the soil has an impact on how well plants absorb nutrients. As a result, both above and below-the-surface water dynamics have an effect on crop growth. The quality of the soil and its mechanical qualities can be significantly altered by both an excess or a lack of water, which could make food production unsustainable. This study deals with the development of a precision farming approach to irrigation that considers the topographical features of the arable land and incorporates its morphological properties. The prediction of the water movement in the topsoil layer is an essential element of this strategy, which uses an agent-based model to describe the soil dynamics and the impact of irrigation and exploits a model predictive control (MPC) to optimize water usage. As a case study, the municipality of Samacá in the department of Boyacá, Colombia, is considered.

1. Introduction

Sustainable food production can be seen as the use of finite resources at a renewable rate. In this context, plants are the principal consumers and moderators of soil and water. For sustainable agricultural practices to be carried out, it is essential to have a thorough understanding of the characteristics and attributes of the soil (Brevik et al., 2016). In-depth maps of the various soil types and their intended uses are needed for this purpose. Pedological and topography data must be combined to develop models that explain how water moves through soil dynamically.

In Colombia, however (and other emerging countries), this type of information is partial and incomplete, and this is why models that allow efficient water use with a minimum set of online information are necessary for large-scale food production (Díaz-González, Rojas-Palma, & Carrasco-Benavides, 2022). That is why this work considers a model that interprets the heterogeneity of cropping land and suggests a water utilization strategy that is efficient in nature, taking the topography of the terrain into account.

A model built using the formalism of partial differential equations should be the best option for accurately interpreting the variation of soil properties throughout the surface, as it captures the continuous evolution of soil physical properties. However, the model derivation and spatial discretization considering realistic geometries is delicate.

This is the motivation behind the adoption of an alternative methodology in this study, which begins with the discretization of the terrain utilizing information extracted from aerial photographs. Every element in the field partition is interpreted as an individual with homogeneous properties which is considered as an agent. The set of all these agents and their interactions in a functional model aiming at the flows of water in the crop field form an agent-based model (ABM).

In Jimenez, Cardenas, Canales, Jimenez, and Portacio (2020), the authors review the use of ABMs to manage agricultural resources. The primary takeaways are the terrain scalability and the flexibility of ABM formulation to satisfy production requirements. In Lopez-Jimenez, Quijano, and Vande Wouwer (2021), the authors propose an ABM capturing the soil heterogeneity and dedicated to the development of irrigation policies.

The present study aims to address two open issues in agriculture. The first problem is to develop an optimal irrigation strategy for a vast land area, taking knowledge about the topography into account. The second problem is to effectively address the trade-off between the cost of water and the benefits of using it for crop cultivation in scenarios of climate change. Climate change, on the one hand, can reduce the amount of available freshwater in areas that were typically used for agriculture and farming, and on the other hand, imply increasing surface water possibly leading to waterlogging. In these cases,

* Corresponding author.

E-mail addresses: jorgelopez@uniandes.edu.co (J. Lopez-Jimenez), nquijano@uniandes.edu.co (N. Quijano), laurent.dewasme@umons.ac.be (L. Dewasme), alain.vandewouwer@umons.ac.be (A. Vande Wouwer).

<https://doi.org/10.1016/j.conengprac.2024.106012>

Received 20 December 2023; Received in revised form 29 June 2024; Accepted 1 July 2024

0967-0661/© 2024 Elsevier Ltd. All rights are reserved, including those for text and data mining, AI training, and similar technologies.

inappropriate irrigation policies can lead to a decrease in agricultural productivity and quality.

Therefore, the main contribution of the present study is to extend the agent-based modeling work of Lopez-Jimenez et al. (2021) with the proposal of an irrigation strategy based on model predictive control (MPC). MPC uses the prediction of the system behavior based on a so-called control-oriented model (COM) and solves at each sampling instant an optimization problem to compute the next control moves (Camacho & Bordons, 2007; Rossiter, 2003). The use of COM, usually in the form of reduced-order models (in contrast with simulation-oriented models (SOM)), allows real-time operation (Alba, 2012). The optimization problem can consider various constraints, including physical, economic, and safety constraints, among others (Qin & Badgwell, 2003; Qin, Badgwell, Allgöwer, & Zheng, 2000). In situations where variable regulation or trajectory tracking is not the main goal, an economic MPC can be used instead, which aims at optimizing the use of resources such as energy and water (or other consumables) as well as the efficiency of the process (Angeli, Amrit, & Rawlings, 2012). The MPC framework has gained significant popularity in various industrial applications, where the process nonlinearity and constraints challenge traditional control strategies to ensure stability and meet multiple performance criteria (Raković & Levine, 2018).

MPC is a versatile framework that allows various goals to be achieved as presented in Balbis (2019), where the controller anticipates crop water demand and maintains optimal soil moisture while reducing water consumption under constrained production budgets. In this way, the MPC approach has been used in a few irrigation applications, where the controller aims to deliver an optimal water quota for homogeneous soils (Ding, Wang, Li, & Li, 2018), or considering multiple layers across the depth and measuring only soil moisture (Lozoya et al., 2014).

Whereas it is not novel to combine ABM and MPC (for example, a multi-agent model predictive control based on resource allocation coordination is presented in Luo, Bourdais, van den Boom, and De Schutter (2017) for a class of hybrid systems with limited information sharing), the combination of MPC and ABM has not been exploited yet in agricultural applications related to crop–soil dynamics, at least to the best of the author’s knowledge.

Moreover, none of the previous works integrates irrigation policy design with models that consider variability across the surface for uneven terrains either based on classical partial differential equation modeling or an alternative approach such as ABM. The effects of long-term agricultural activity can deteriorate the composition and consistency of the soil due to over-irrigation or erosion (Eekhout, Hunink, Terink, & de Vente, 2018). These effects can be accentuated due to climate change, which is why irrigation systems are required to incorporate climate variability to guarantee efficiency and sustainability (Berg & Sheffield, 2018).

Hence, in this study, an ABM model is exploited to interpret the soil variability across the surface and take water flows into account (Lopez-Jimenez et al., 2021). This model is extended to incorporate the negative effects of excess water in the soil, which can be part of the problems arising in a climate change context, and is used as a predictor in a model predictive control strategy that considers limited water resources for the duration of the crop cycle. MPC can be fed with information regarding on-field measurements as well as weather forecasts.

This paper is organized as follows. In Section 2, the construction of the predictive model considering soil variability is detailed, while the economical MPC strategy is presented in Section 3. Afterward, in Section 4, the case study related to the municipality of Samacá in the department of Boyacá, Colombia, is presented. Finally, Section 5 draws conclusions and perspectives.

2. Predictive model

The model is based on two components: a procedure to extract information about the terrain from imaging data and a model incorporating terrain variability and predicting water flows.

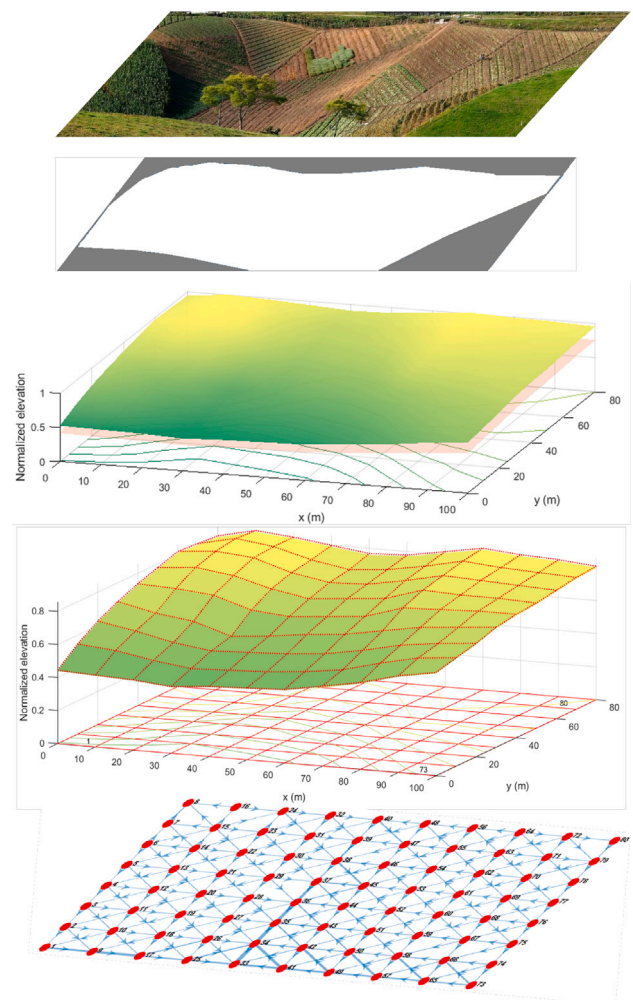


Fig. 1. Building of DEM, grid layout, and a directed graph representing agent assignment and location.

2.1. Extraction of terrain information

The acquisition system used in this work is mostly based on aerial images to collect information about land topography and water movement. Additionally, on-field sample measurements and data extracted from geographic information system (GIS) software are complementary sources of information. Once the target terrain is chosen, a set of medium-resolution imagery is collected and processed as follows according to Fig. 1:

1. Selection of the geographic location of the target field.
2. Merge of images to shape the full field.
3. Delimitation of boundaries and frontiers of the target field.
4. Edge detection and field image segmentation.
5. Construction of a digital elevation model (DEM).
6. Grid plot based on the terrain heterogeneity.
7. Assignment of an identifier to each cell in the grid and construction of the directed graph and adjacency matrix.

The image processing and mapping tools used in this study are open access, such as OpenCV (Bradski & Kaehler, 2008; Sheshadri, Dann, Hueser, & Scherberger, 2020; Yu, Cheng, Cheng, & Zhou, 2004) for image processing, and QGIS (Kurt Menke, Smith, Pirelli, John Van Hoesen, et al., 2016; Moyroud & Portet, 2018), to build the DEM model.

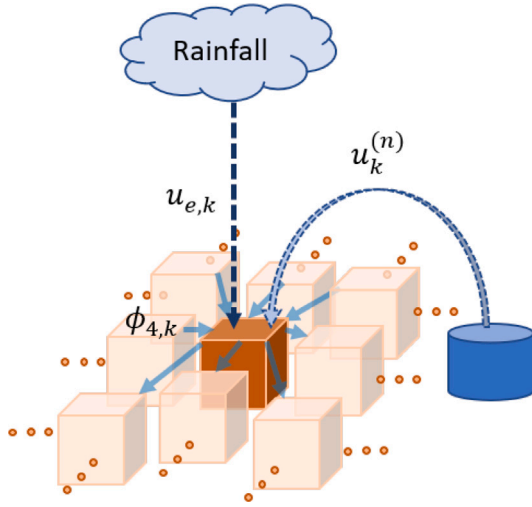


Fig. 2. Conceptual diagram of the ABM for predicting water flows in the soil, with $n = 1, \dots, N$, crop–soil agents. A sample agent is highlighted with ϕ_4 the incoming water from higher-level neighbors, u_e the rainfall, and $u^{(n)}$ the irrigation input. The subindex k corresponds to the time evolution index.

2.2. Prediction of water flows

After the grid is deployed over the terrain and the grid cells have been assigned a label, each cell becomes an agent. Therefore, the collection of agents composes the ABM, as described in Lopez-Jimenez et al. (2021)

The ABM considered in this study aims to forecast the evolution of crop–soil water content and biomass based on local data from a limited number of sensors. Hence, two types of agents are proposed. The first relates to a region of uniform soil with a regular-shaped surface, and the second is intended for irrigation management. There are as many crop–soil agents as grid patches, however, there is only one irrigation agent that interacts directly with all the crop–soil agents.

This research assumes that while irrigation may either follow a predetermined strategy or be turned off, the main driving factor for crop growth is the environmental inputs such as rain. This means that even without irrigation, the crop evolves to maturity, but irrigation provides an external way to change the crop’s dynamic behavior.

This model is particularly well suited to simulate crop landscapes with rough topography where the interactions between crop–soil agents are provided by water exchanges. Fig. 2 shows the conceptual representation of the discretized land surface and highlights a sample agent and the main water inputs and outputs.

The mathematical structure of each crop–soil agent is composed of a set of four discrete dynamical equations. The first equation represents the evolution of water content in the soil. The second one is the accumulation of thermal energy. The third one accounts for the aging of the crop to maturity, including reducing stress factors related to extreme environmental inputs. The fourth equation explains biomass growth and reductive factors, including thermal and hydric stresses. Thus, the dynamical equations are:

$$x_{1,k+1}^{(n)} = x_{1,k}^{(n)} - \phi_{1,k}^{(n)} - \phi_{2,k}^{(n)} - \phi_{3,k}^{(n)} + \phi_{4,k}^{(n)} + u_{e,k}^{(1)} + u_k^{(n)} \quad (1a)$$

$$x_{2,k+1}^{(n)} = x_{2,k}^{(n)} + h_{1,k}^{(n)} \quad (1b)$$

$$x_{3,k+1}^{(n)} = x_{3,k}^{(n)} + \theta_{11}^{(n)}(1 - h_{2,k}^{(n)}) + \theta_{12}^{(n)}(1 - h_{3,k}^{(n)}) \quad (1c)$$

$$x_{4,k+1}^{(n)} = x_{4,k}^{(n)} + \theta_{13}^{(n)} h_{6,k}^{(n)} h_{7,k}^{(n)} h_{8,k}^{(n)} g_k^{(n)} u_{e,k}^{(4)}. \quad (1d)$$

For the water in the soil (Eq. (1a)), the mass balance equation considers the input fluxes of water due to rainfall ($u_{e,k}^{(1)}$), irrigation ($u_k^{(n)}$)

and excess from higher-level neighbors ($\phi_{4,k}^{(n)}$), and outgoing fluxes given by the crop transpiration ($\phi_{1,k}^{(n)}$) which includes the reference evapotranspiration, the surface runoff ($\phi_{2,k}^{(n)}$) which accounts for physical soil characteristics, and the deep drainage ($\phi_{3,k}^{(n)}$), which considers the soil mechanical properties to hold water. Besides, the accumulation of thermal energy (Eq. (1b)) includes the air temperature as conditional input given in $h_{1,k}^{(n)}$. The third equation that accounts for the aging of the crop to maturity (Eq. (1c)) includes heat stress ($h_{2,k}^{(n)}$) and drought stress ($h_{3,k}^{(n)}$). Finally, the biomass equation (Eq. (1d)) gathers waterlogging stress ($h_{6,k}^{(n)}$), low temperature stress ($h_{7,k}^{(n)}$), CO_2 growth contribution factor ($h_{8,k}^{(n)}$), a growth function ($g_k^{(n)}$) and solar radiation ($u_{e,k}^{(4)}$). A summary of the key components of the models is presented next, while a complete list of functions, variables, and parameters is described in Lopez-Jimenez et al. (2021).

The crop transpiration $\phi_{1,k}$ is given by

$$\phi_{1,k} = \min(\theta_1(x_{1,k} - \theta_2\theta_5), u_{e,k}^{(2)}), \quad (2)$$

where θ_1 is the water uptake coefficient, θ_2 is the wilting point, θ_5 is the root-zone depth, and $u_{e,k}^{(2)}$ is the reference evapotranspiration.

The surface runoff $\phi_{2,k}$ is computed as

$$\phi_{2,k} = \begin{cases} \frac{(u_{e,k}^{(1)} - \theta_3)^2}{(u_{e,k}^{(1)} + 4\theta_3)}, & u_{e,k}^{(1)} > \theta_3 \\ 0, & u_{e,k}^{(1)} \leq \theta_3, \end{cases} \quad (3)$$

where θ_3 is the initial abstraction. The deep drainage $\phi_{3,k}$ is estimated as

$$\phi_{3,k} = \begin{cases} \theta_4(x_{1,k} + u_{e,k}^{(1)} - \phi_{2,k} - \theta_6\theta_5), & x_{1,k} + u_{e,k}^{(1)} - \phi_{2,k} > \theta_6\theta_5 \\ 0, & x_{1,k} + u_{e,k}^{(1)} - \phi_{2,k} \leq \theta_6\theta_5, \end{cases} \quad (4)$$

where θ_4 is the drainage coefficient, and θ_6 is the field capacity.

The function $h_{1,k}$ represents the daily mean temperature added to the state variable $x_{2,k}$, i.e.,

$$h_{1,k} = \begin{cases} u_{e,k}^{(3)} - \theta_7, & u_{e,k}^{(3)} > \theta_7 \\ 0, & u_{e,k}^{(3)} \leq \theta_7, \end{cases} \quad (5)$$

where $u_{e,k}^{(3)}$ is the mean air temperature and θ_7 is the base temperature for phenology development and growth. The heat stress $h_{2,k}$ is computed as follows

$$h_{2,k} = \begin{cases} 1, & u_{e,k}^{(6)} \leq \theta_9 \\ 1 - \frac{u_{e,k}^{(6)} - \theta_9}{\theta_{10} - \theta_9}, & \theta_9 < u_{e,k}^{(6)} \leq \theta_{10} \\ 0, & u_{e,k}^{(6)} > \theta_{10}, \end{cases} \quad (6)$$

where θ_9 is the threshold temperature to start accelerating senescence from heat stress, θ_{10} is the extreme temperature threshold when radiation use efficiency (RUE) becomes 0 due to heat stress, and $u_{e,k}^{(6)}$ is the maximum daily temperature.

The drought stress $h_{3,k}$ can be expressed as

$$h_{3,k} = 1 - \theta_{14} h_{4,k}, \quad (7)$$

where θ_{14} is the sensitivity factor to radiation-use efficiency, and

$$h_{4,k} = \begin{cases} 1 - \frac{\phi_{1,k}}{u_{e,k}^{(2)}}, & \phi_{1,k} < u_{e,k}^{(2)} \\ 0, & \phi_{1,k} \geq u_{e,k}^{(2)}. \end{cases}$$

The incoming flux $\phi_{4,k}$ is computed as the sum of the outflows $\phi_{out,k}$ from all the neighbors, which have a normalized elevation γ higher than the considered agent. The outflow of such an agent is given by

$$\phi_{out,k} = \begin{cases} \frac{(x_{1,k} - \theta_6\theta_5) + \phi_{2,k}}{N_r}, & x_{1,k} > \theta_6\theta_5 \\ 0, & x_{1,k} \leq \theta_6\theta_5, \end{cases} \quad (8)$$

Table 1

General notation used throughout this work.

N	Number of agents
$n = 1, \dots, N$	Index of agents
k	Time index
t_h	Harvest time
x_1	Water content in soil
x_2	Cumulative temperature
x_3	Cumulative temperature until maturity to reach 50% radiation interception
x_4	Biomass
u	Irrigation
$u_e^{(1)}$	Rainfall
$u_e^{(3)}$	Mean air temperature
$u_e^{(4)}$	Solar radiation
$u_e^{(6)}$	Maximum daily temperature
ϕ_1	Crop transpiration
ϕ_2	Surface runoff
ϕ_3	Deep drainage
ϕ_4	Incoming flux from neighbors
h_1	Mean temperature
h_2	Heat stress
h_3	Drought stress
h_6	Waterlogging stress
h_7	Low temperature stress
h_8	CO ₂ growth contribution factor
g	Growth function
θ_{11}	Heat stress parameter
θ_{12}	Drought stress parameter
θ_{13}	Radiation use efficiency
λ	Weighting factor of cost function
$\gamma^{(n)}$	Normalized elevation

where N_r is the number of receiving neighbors, and θ_6 is the field capacity. Finally, the growth function g_k^n is given by

$$g_k^n = \begin{cases} \frac{\theta_{19}}{1+e^{-0.01(x_{2,k}-\theta_{20})}}, & x_{2,k} \leq \frac{\theta_{18}}{2} \\ \frac{\theta_{19}}{1+e^{0.01(x_{2,k}+x_{3,k}-\theta_{18})}}, & x_{2,k} > \frac{\theta_{18}}{2}, \end{cases} \quad (9)$$

where θ_{18} is the cumulative temperature requirement from sowing to maturity, θ_{19} is the maximum fraction of radiation interception that a crop can reach, and θ_{20} is the cumulative temperature requirement for leaf area development to intercept 50% of radiation. Table 1 provides a summary of the parameters and variables.

3. Design of an irrigation policy

As previously mentioned, the evolution of crop–soil agents is governed by environmental inputs and soil conditions. Climatic inputs can accelerate or retard plant growth, while soil conditions determine the amount of water available for each crop agent. Additionally, the agents model the positive and negative effects of water scarcity and excess on plant growth, regardless of whether the water comes from irrigation, rain, or neighbors on higher ground. Considering water as the main driving input of the model, it can be supplied either by rain or irrigation. Nevertheless, in formulating the irrigation strategy, rainfall is considered an uncontrollable factor, and irrigation is controllable, where the soil and the plants act as elements of water storage and consumption.

According to these assumptions, the design of the irrigation policy starts from the evaluation of the behavior of the crop under ideal conditions of water availability to determine the maximum amount of water necessary for every agent during the full crop cycle. Once the ideal water quota is computed, the problem can be constrained to realistic scenarios where water is scarce and expensive. The amount of water needed for the full crop lifetime is defined as W_{tot} . A lower value of W_{tot} could drive drought stress, and an upper value could drive waterlogging stress for some lapses of the growing cycle. In any case, the crop yield diminishes, but in the case of overuse of water, the losses

increase due to the costs of water and irrigation processes. The ideal amount of water in soil is related to the water in the root zone which means that this value must be above the wilting point and below the field holding capacity. For practical purposes in this work, the field holding capacity is considered as the ideal water amount in the soil.

Then, the objective function is composed of the combination of two criteria: the average growth and the weighted average of irrigation quota. Therefore, the irrigation strategy combines two goals. On the one hand, a maximization of the agent’s individual growth considering the positive and negative water effects, and on the other hand, minimization of the water use due to availability and relative cost.

To achieve this objective, the problem is subject to the water exchanges that occur every day due to the land’s topography, the water consumption by plants, the soil dynamics, and the availability of irrigation water for every agent during the crop cycle. Also, the policy considers that rain can significantly affect the amount of water available for each agent positively or negatively since both waterlogging and drought can decrease crop yield. Consequently, the irrigation policy is defined by the solution to the following optimization problem:

$$\min_{u^{(n)}} J(u^{(n)}) = -\frac{1}{N} \sum_{n=1}^N \frac{x_4^{(n)}(H_p)}{x_{4,max}(H_p)} + \lambda \sum_{k=1}^{H_p} \sum_{n=1}^N \frac{u^{(n)}(t_k)}{W_{maxH_p}(t_k)} \quad (10a)$$

$$\text{s.t.} \quad \sum_{k=1}^{H_p} \sum_{n=1}^N u^{(n)}(t_k) \leq W_{maxH_p}(t_k) \quad (10b)$$

$$\sum_{k=1}^{H_p} x_1^{(n)}(t_k) \leq W_{fc}^{(n)} \quad (10c)$$

$$0 \leq u^{(n)}(t_k) \leq U_B \quad \forall n = 1, \dots, N \quad (10d)$$

$$x_1^{(n)}, x_2^{(n)}, x_3^{(n)}, x_4^{(n)} \text{ are given by (1)} \quad (10e)$$

$$W_{maxH_p}(t_k + 1) = W_{tot} - \sum_{n=1}^N u^{(n)}(t_k) \quad (10f)$$

where N is the number of soil patches, H_p is the prediction horizon which cannot be greater than the harvest time t_h , $x_4^{(n)}(H_p)$ is the biomass of the agent n at the prediction horizon lapse, λ is a weighting factor between biomass growth and water expense, $u^{(n)}(t_k)$ is the irrigation of patch n at day k , $x_1^{(n)}(t_k)$ is the water in the soil for agent n at time k , $W_{fc}^{(n)}$ is the water at field capacity for each agent, U_B is the vector of maximum water allowed for irrigation each day, and $W_{maxH_p}(t_k)$ is the maximum amount of water available for the prediction horizon H_p . As the model is driven by environmental inputs that cannot be known in advance, the selection of the prediction limit H_p is based on the typical weather forecast horizons for climatic variables (i.e., from 2 to 30 days).

The amount of effective water used every day ($\sum_{n=1}^N u^{(n)}$) is discounted from W_{tot} each time the algorithm is executed and consequently can limit $W_{maxH_p}(t_k)$.

In practice, the rationale behind the selection of lambda relies on the relative value of water in the local context of the crop field, i.e., the cost of freshwater as compared to the potential market value of the biomass produced. The selection of the prediction horizons is linked to practical constraints. For instance, daily irrigation can increase the logistic costs associated with the deployments of irrigation machinery, while large prediction horizons can be undermined by the uncertainty in the weather forecast.

Note that the objective function $J(u^{(n)})$ is always continuous on the prediction horizon H_p . Moreover, the inclusion of this horizon in the constraints guarantees the feasibility of the optimization problem. However, the nonlinearities and discontinuities of the model (i.e., $\phi_1, \phi_2, \phi_3, \phi_4, h_1, h_2, h_3, h_6, h_7$ are piece-wise functions, and g is nonlinear and piece-wise) limit the use of methods for solving the optimization problem based on derivatives (e.g., some algorithms included in the *fmincon* function of Matlab). However, in this work, the *interior-point*

Table 2
Comparative results for no irrigation, fixed irrigation schedule, soil moisture-based irrigation, and MPC-based irrigation policy for the four climatic scenarios.

	Strategy	Irrigation per agent (mm)	Water saving	Biomass (ton/Ha)	Biomass increase
Scenario 1 (heavy rainy season)	No irrigation	0	0%	1707.81	0%
	Fixed Irrigation (15mm)	120	0%	1770.63	4%
	Soil moisture irrigation	232	-94%	1657.63	-3%
	MPC ($H_p = 8 \lambda = 0.01$)	39	68%	1870.63	10%
Scenario 2 (dry season)	No irrigation	0	0%	1423.88	0%
	Fixed Irrigation (15mm)	120	0%	1648.69	16%
	Soil moisture irrigation	413	-244%	1735.75	22%
	MPC ($H_p = 8 \lambda = 0.01$)	51	58%	1774.31	25%
Scenario 3 (consistent rainfall)	No irrigation	0	0%	1201.38	0%
	Fixed Irrigation (15mm)	120	0%	1411.38	17%
	Soil moisture irrigation	395	-229%	1580.00	32%
	MPC ($H_p = 8 \lambda = 0.01$)	38	68%	1649.63	37%
Scenario 4 (rainy beginning and dry end)	No irrigation	0	0%	1666.00	0%
	Fixed Irrigation (15mm)	120	0%	1764.06	6%
	Soil moisture irrigation	319	-166%	1712.69	3%
	MPC ($H_p = 8 \lambda = 0.01$)	47	61%	1834.19	10%

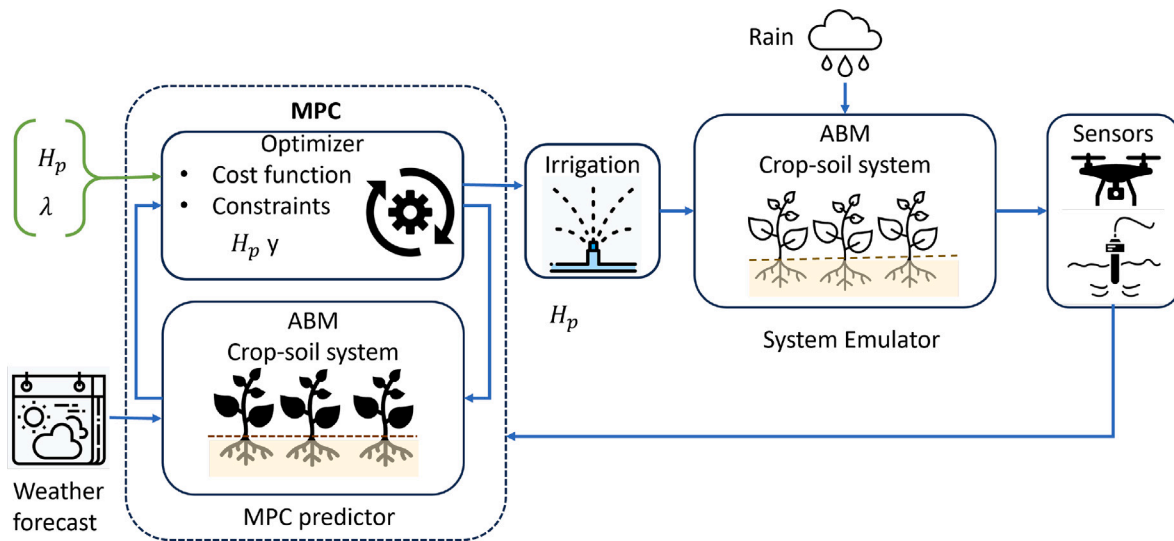


Fig. 3. Model predictive control scheme proposed to implement the irrigation policy.

algorithm is selected, and its feasibility is verified for all ranges of the parameters of the optimization problem (i.e., prediction horizon, number of agents, and λ values).

The implementation of this irrigation policy is based on the model predictive controller framework proposed by Lozoya, Mendoza, Aguilar, Román, and Castelló (2016). In Lozoya et al. (2016), the authors used a soil moisture model to emulate the process dynamics and as a component of the MPC predictor. In the present study, the ABM model given by (1) is used either as the MPC predictor and the crop-soil system emulator (See Fig. 3). In this scheme, the dynamics associated with the water application mechanism are neglected, and irrigation is applied ideally in the geographical location required according to the schedule given by the optimizer.

As illustrated in the flow diagram of Fig. 4, the process begins with the selection of the field and crop characteristics as it conditions the parameters of the ABM, particularly the soil composition and mechanical properties such as the water-holding capacity and the wilting point. Next, the setup of the MPC includes the selection of values for λ , H_p , and the amount of water available for the entire crop development period (i.e., W_{max}). An iterative cycle then starts to minimize the cost function over the prediction horizon (H_p) under the condition that some water is still available within the budget. The irrigation quota is then computed and applied to the ABM. Otherwise, the ABM is

executed until the cropping period's end without the irrigation quota computation.

In this simulation study, the environmental inputs come from a synthetic database described in the case study. In a real application, the data feeding the MPC predictor should come from a weather forecast source.

In practice, irrigation of large fields involves complex logistics and deploying equipment that cannot be modified or rescheduled quickly (e.g., pumps, hoses, pipes, valves, structures that support sprinklers, and irrigation actuators). In addition, when considering implementing a management system, it is important to consider the economic feasibility of adopting the optimal irrigation strategy. Factors such as investment costs, water savings, and agricultural yield improvements should be considered. The publications by Lehmann and Finger (2014) and Ishfaq et al. (2022) propose approaches to tackle these economic difficulties. The proposed control framework should provide a decision tool to establish an irrigation schedule over a typical management time frame. This is a supporting reason to choose a prediction horizon ranging from 2 to 30 days. Depending on the flexibility of the irrigation resources, the MPC strategy can generate the irrigation policy in real time and enhance water management and resource allocation.

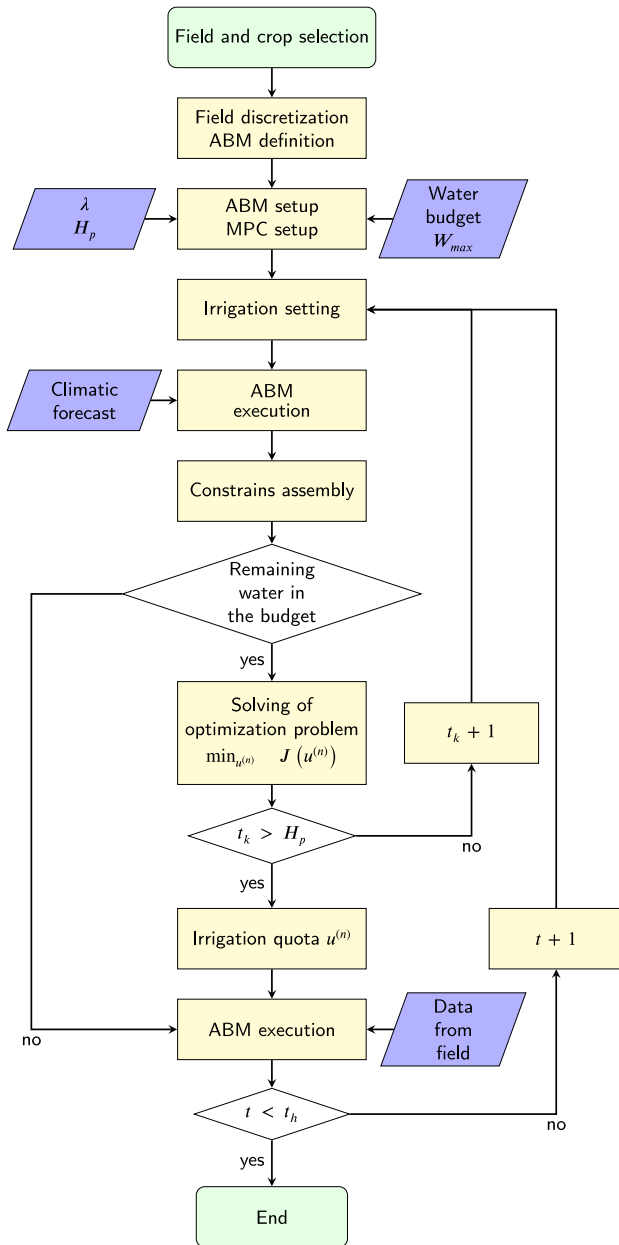


Fig. 4. Flowchart of the algorithm for the ABM-MPC.

4. Case study

As a case study, a rugged terrain is selected and used as a testbed under four climatic scenarios to assess the water in soil behavior following environmental changes (mainly rainfall) (see Fig. 5). The testbed is located near Samacá in the state of Boyacá, Colombia, between 2400 and 2800 m.a.s.l. (meters above sea level). The parcel has a square shape of 400 by 400 m and well-defined high and low parts as shown in Fig. 6 that comprehensively represent water movement due to topographic changes and agricultural activities. The soil is mostly loamy sandy and the root zone depth (i.e., topsoil) has a thickness between 300 to 500 mm. The grid partition of the field is based on the resolution of available aerial images. Additionally, environmental conditions are assumed to be the same for the entire crop area.

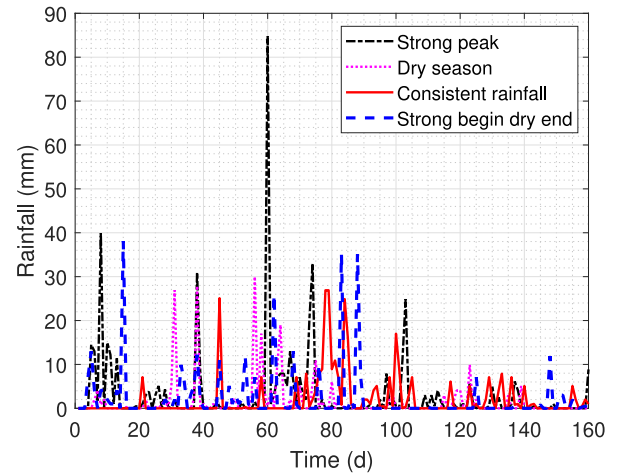


Fig. 5. Climatic scenarios, (a) heavy rainy season with strong peaks; (b) dry season, (c) consistent rainfall, and (d) rainy beginning and dry end. The accumulated quantities of rainfall for the four scenarios are 483 mm, 244 mm, 322 mm, and 325 mm, respectively.

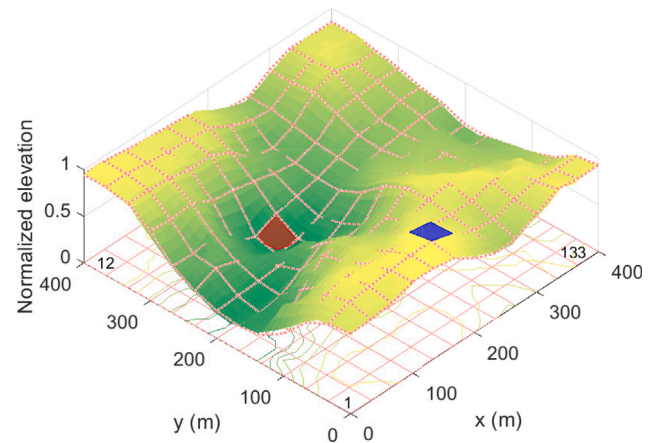


Fig. 6. 3D elevation model of the test field with grid partition. The patches of the highest and lowest agents are displayed in blue and red respectively.

A few base reference cases are first defined. The first ones correspond to the different rain patterns in the four considered climatic scenarios with no irrigation policy. The next ones envision two basic irrigation strategies commonly used by small farmers. The first one is a fixed irrigation schedule based on farmers' expertise about the crop, focused on the germination stage and relaxed on the growing stage. The second one uses simple probes to measure soil moisture to ensure water feeding to reach field capacity. The results are shown in Fig. 7 and serve as the evaluation basis of the MPC results, which are discussed in the next section (See Table 2).

4.1. Unconstrained irrigation policy

The first tests consist of evaluating the optimal irrigation policy (i.e., Eq. (10a)) without considering restrictions regarding the total amount of water (i.e., Eq. (10b)), the amount of water that can be applied to each agent (i.e., Eq. (10d)) and the water holding capacity of each agent (i.e., Eq. (10c)).

The assessment of crop–soil closed-loop performance for different values of the irrigation policy design parameters (i.e., λ and

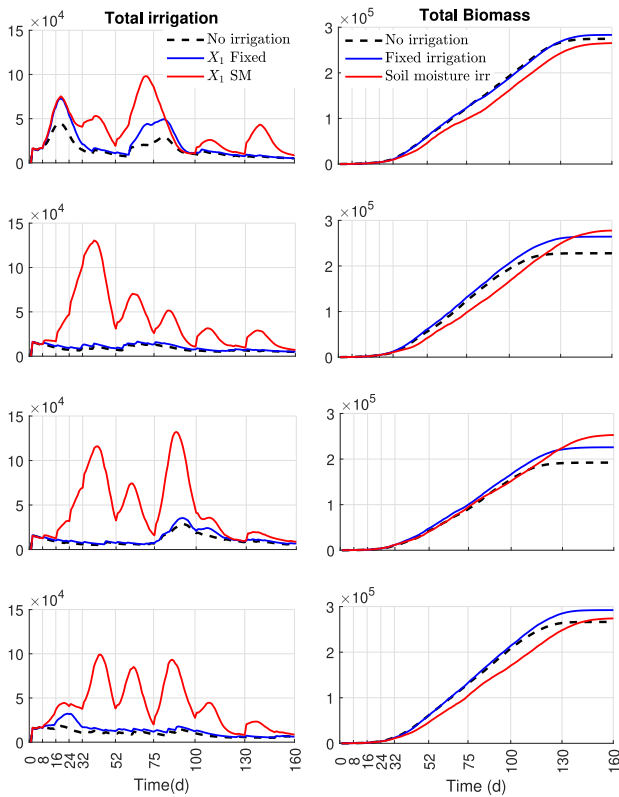


Fig. 7. Comparative performance of the total water in soil and biomass for the full set of agents when no irrigation, fixed irrigation scheduling, and the soil moisture irrigation strategy are applied. Both irrigation strategies are enforced on days 8, 16, 24, 32, 52, 75, 100, and 130. The irrigation quota per day in the fixed strategy is 15 mm. From top to bottom, the results are for: (a) heavy rainy season with strong peaks; (b) dry season, (c) consistent rainfall, and (d) rainy beginning and dry end.

H_p) provides an insight into soil dynamics highlighted by the water in soil (x_1) and biomass (x_4). Fig. 8 shows the results for $\lambda \in \{0.0001, 0.001, 0.01, 0.1, 1\}$ and $H_p \in \{3, 8, 14\}$ during the strong peak scenario. The positive effect of considering more days for the prediction horizon is evidenced by the reduction of the negative water stress that limits biomass production by the agents located in the lowest parts of the field. The same effect occurs for other climatic scenarios since soil dynamics allow for water exchanges.

However, the extension of the prediction horizon to account for the climatic effect on the irrigation schedule cannot improve the maximization of biomass production since the output water fluxes of the agents located in lower terrains are slower than the incoming ones. For instance, rainfall or runoff from higher locations can have an impact in minutes but drainage or evaporation can take hours or even days. Moreover, as the model considers the negative effect of water excess on the entire field, it is clear that the sole pursuit of maximizing the biomass of higher agents is hampered by the same objective for lower ones. The effect is more critical when the crop develops in a heavy rainy season, but it can also be noticed in a dry season under over-irrigation.

The positive effect of a large prediction horizon is shown in Fig. 9, for all climate scenarios with $\lambda = 0.1$. Notice that total irrigation decreases as H_p becomes larger. However, a rise occurs with $H_p = 5$ during the strong beginning/dry end case. Indeed, at the beginning of the crop span, the model cannot discriminate if the adverse effect comes from an excess or a lack of water since the crop growth over the surface occurs 20 days after seeding. Moreover, if the prediction horizon is short (e.g., $H_p = 3$) the optimizer becomes highly sensitive to rain disturbances.

The penalization of water usage given by λ helps reduce water over-application on the entire field. This statement is more dramatic

for agents with high water exchange rates due to their topographic location, but it is not sufficient to contribute to the reduction of negative effects during the rainy season.

4.2. Irrigation policy with water constraints

In the optimization problem, there are two ways to incorporate the constraints related to the available amount of water. The first one consists of managing a fixed amount of water for the entire crop cycle and all agents (Eq. (10b)). The second one is to restrict the maximum amount of water dedicated to each agent (Eq. (10d)).

The best results are obtained with $H_p = 14$ and $\lambda = 0.1$, which provide equal relevance to the production of biomass and the cost of water as shown in Fig. 10. Notice that even with a good performance of the extremely located agents, driven by the optimization process, there are intermediate agents suffering from the side effects of multiple water exchanges. Fig. 10 shows the performance of the full set of crop-soil agents, highlighting the ones located in the highest and lowest parts of the field.

Applying the optimal irrigation policy leads to a global increase in crop yield. The average production ranges from 1960 to 2130 tons/Ha, representing a production increase of around 9% (for scenario a). Regarding the other climate scenarios (i.e., b, c, and d), not shown in the graph, the production increases are 28%, 15%, and 12%, respectively. The highest benefit of applying the optimal irrigation policy is achieved in seasons with low rainfall since the system can better manage the negative effects of excess water in the lower parts of the land. However, the above benefit will only be possible if enough water is available for the crop life span.

The ideal amount of water for each of the agents is quantified by the ABM (Equation (1)), and the addition of all the individual-agent amounts gives the maximum level for the entire crop (i.e., W_{tot}). This amount of water is ideal because it maximizes production, preventing each agent from suffering from a shortage or excess of water. However, due to the crop dynamics given by the geographic position of each agent (compiled in the graph), some of them may reach a stress level for short periods. Additionally, since rain is unavoidable, there will be more water available. That said, when W_{tot} is constrained to 90%, there are no significant changes in production for any of the four scenarios. However, when the reduction is between 90% to 70%, the change in biomass is below 5% in all scenarios. Moreover, when irrigation is strongly limited below 70% the crop yield diminishes by about 30 to 40%, particularly in the second scenario.

To illustrate the restriction of W_{tot} to 75% for the second climatic scenario, an upper bound of 5 mm of water per agent is enforced (see Fig. 11). In this case, the daily limitation contributes to ensuring water availability during all phenological stages, guaranteeing that the drop in crop yield is never greater than 5%.

The application of the irrigation policy increases, on average, the total production by about 15%. However, for the agents located in the lower parts, the production is drastically lower due to the adverse effects of waterlogging. To mitigate this negative effect, the prediction horizon can be extended. Another option may be to design an irrigation policy that combines the objective of maximizing production and minimizing the stress caused by waterlogging. However, this option depends on the sensing system, since it requires having complete information on the stress suffered by the plants, whether due to drought or waterlogging.

In summary, it is more beneficial to limit the maximum amount of water that may be provided to each agent and distribute water over a longer time when the water budget is constrained. The irrigation scheme provides more water at the start of the crop span when only the total amount of water is limited until the resource is depleted. The crop's ability to rely only on rainfall reduces crop yield.

A comparative evaluation of the MPC irrigation policy with the two basic irrigation strategies is presented in Table 2. The water savings

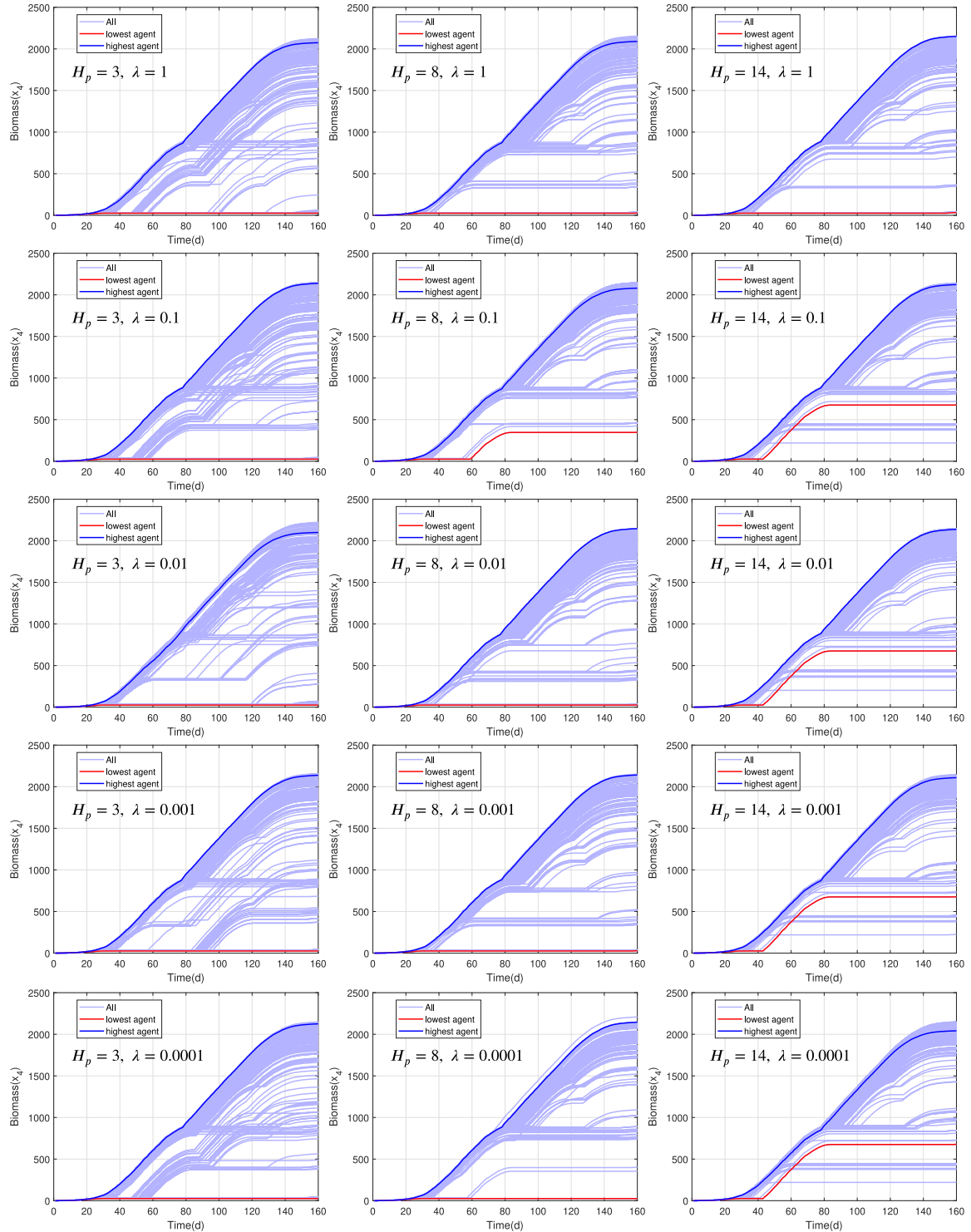


Fig. 8. Assessing the impact of λ on biomass for all agents under strong peak scenario for prediction horizons of $H_p = 3, H_p = 8,$ and $H_p = 14$ days.

are computed considering the fixed irrigation scheme as the reference, whereas the biomass increase is computed considering the no irrigation case as the reference. The prediction horizon is fixed at 8 days to present a fair comparison. All irrigation strategies can increase the biomass in dry or low rainy scenarios. However, only the MPC strategy can increase biomass production while keeping water savings. The biomass increase ranges from 10 to 37%, whereas the water savings

range from 58 to 68%. Therefore, the main advantage of the optimal irrigation policy is a satisfactory increase in biomass production while keeping water usage at a minimum due to the incorporation of the positive and negative effects of water in the ABM.

Regarding the optimizer, the computational load varies from milliseconds to several days (e.g., when considering $H_p = 30$ days). This depends on the number of operations and cycles within the machine,

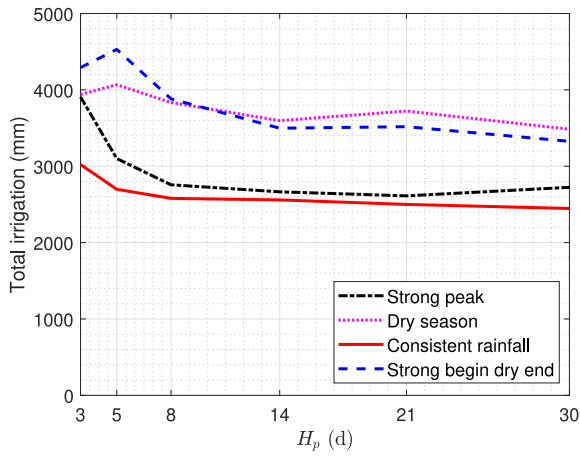


Fig. 9. Total amount of water used for irrigation for $H_p = 3, 5, 8, 14, 21, 30$ days, and $\lambda = 0.1$.

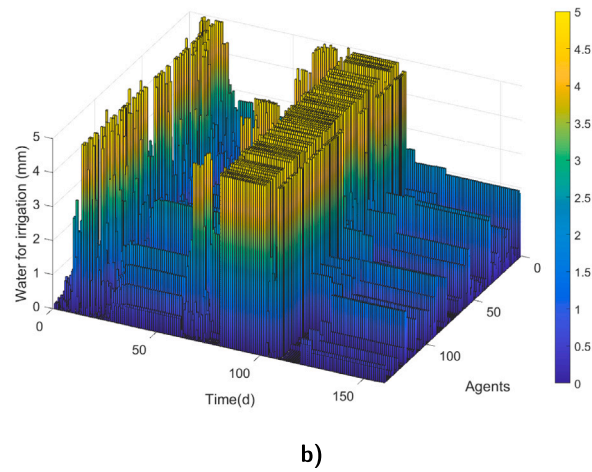
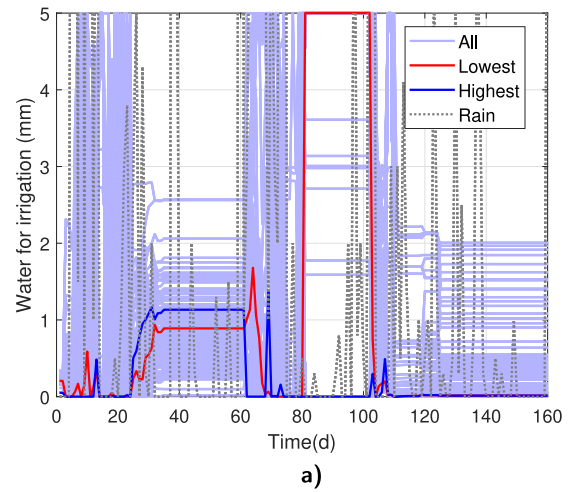


Fig. 11. Irrigation input for all agents for the dry season (i.e., second climatic scenario), (a) highlighting the highest and lowest position and (b) displaying the individual irrigation profile for $H_p = 8$ and $\lambda = 0.1$.

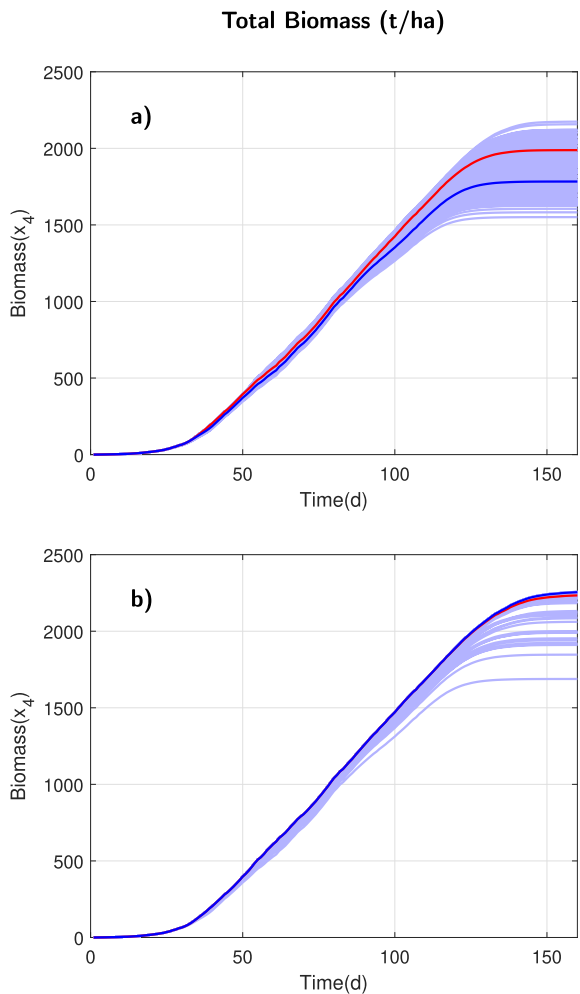


Fig. 10. Biomass performance of all agents during a strong rainy season considering the cases where (a) no irrigation, and (b) irrigation is applied. The behavior of the highest and lowest agents are highlighted in blue and red, respectively.

which are related to diverse factors such as the number of agents N and the forecast horizon H_p . After evaluating the problem in the different scenarios and changing the prediction horizon, the algorithm can converge into an efficient irrigation policy. Nevertheless, the constrained

optimization algorithm is the main limitation of the method to be used in real-time applications.

5. Conclusions

This work proposes an optimal irrigation policy to address the problem of efficient water distribution over uneven terrains. To implement such an irrigation strategy, we propose using model predictive control with an agent-based model as a predictor and formulating resource constraints. The objective function combines two conflicting criteria. The first one maximizes biomass, whereas the second one minimizes water use.

To compute biomass production on an uneven crop field, the first step is to account for soil and land heterogeneity. To this end, a grid discretization of the land surface is used, where each portion or patch corresponds to an agent. Thus, an agent is assumed to be a portion of homogeneous land (both in soil characteristics and relative elevation from its neighbors), and the combination of agents leads to an Agent-Based Model (ABM). On each patch, crop growth is driven mainly by water from environmental or artificial sources. Therefore, the ABM accounts for all water exchanges between neighbors and the impact of either positive or negative effects (i.e., drought and waterlogging) of water on crops growing in each crop-soil agent, subject to diverse environmental scenarios. Moreover, MPC can easily incorporate weather forecasts.

The irrigation strategy is tested in simulation and effectively saves water in different weather scenarios. However, additional case studies should be analyzed to assess the strategy more globally in terms of sustainability and also in the context of varying precipitation patterns and temperatures, such as those induced by climate changes.

Future research and development can go in several directions, such as the development of software sensors that use the ABM model in conjunction with data sources to reconstruct missing information, the design of sensor placement algorithms to find the optimal arrangement of instruments as recently proposed by the authors in Lopez-Jimenez, Quijano, and Vande Wouwer (2023), and, of course, field trials of the proposed methods.

CRedit authorship contribution statement

Jorge Lopez-Jimenez: Writing – original draft, Software, Methodology, Investigation, Formal analysis, Conceptualization. **Nicanor Quijano:** Writing – review & editing, Validation, Supervision, Methodology. **Laurent Dewasme:** Validation, Software. **Alain Vande Wouwer:** Writing – review & editing, Supervision, Methodology, Conceptualization.

Declaration of competing interest

The authors declare that they have no known competing financial interests or personal relationships that could have appeared to influence the work reported in this paper.

References

- Alba, C. (2012). Model predictive control. *Advanced textbooks in control and signal processing*. Springer London.
- Angeli, D., Amrit, R., & Rawlings, J. B. (2012). On average performance and stability of economic model predictive control. *IEEE Transactions on Automatic Control*, 57(7), 1615–1626.
- Balbis, L. (2019). Economic model predictive control for irrigation systems. In *Proceedings of the 2019 8th international conference on modeling simulation and applied optimization* (pp. 1–4). IEEE.
- Berg, A., & Sheffield, J. (2018). Climate change and drought: The soil moisture perspective. *Current Climate Change Reports*, 4(2), 180–191.
- Bradski, G., & Kaehler, A. (2008). *Learning OpenCV: Computer vision with the OpenCV library*. O'Reilly Media, Inc.
- Brevik, E. C., Calzolari, C., Miller, B. A., Pereira, P., Kabala, C., Baumgarten, A., et al. (2016). Soil mapping, classification, and pedologic modeling: History and future directions. *Geoderma*, 264, 256–274.
- Camacho, E. F., & Bordons, C. (2007). Model predictive controllers. In *Model predictive control* (pp. 13–30). London: Springer London.
- Díaz-González, V., Rojas-Palma, A., & Carrasco-Benavides, M. (2022). How does irrigation affect crop growth? A mathematical modeling approach. *Mathematics*, 10(1), 151.
- Ding, Y., Wang, L., Li, Y., & Li, D. (2018). Model predictive control and its application in agriculture: A review. *Computers and Electronics in Agriculture*, 151, 104–117.
- Eekhout, J. P., Hunink, J. E., Terink, W., & de Vente, J. (2018). Why increased extreme precipitation under climate change negatively affects water security. *Hydrology and Earth System Sciences*, 22(11), 5935–5946.
- Ishfaq, M., Akbar, N., Zulfiqar, U., Ali, N., Shah, F., Anjum, S. A., et al. (2022). Economic assessment of water-saving irrigation management techniques and continuous flooded irrigation in different rice production systems. *Paddy and Water Environment*, 1–14.
- Jimenez, A.-F., Cardenas, P.-F., Canales, A., Jimenez, F., & Portacio, A. (2020). A survey on intelligent agents and multi-agents for irrigation scheduling. *Computers and Electronics in Agriculture*, 176, Article 105474.
- Kurt Menke, G., Smith, R., Jr., Pirelli, L., John Van Hoesen, G., et al. (2016). *Mastering QGIS*. Packt Publishing Ltd.
- Lehmann, N., & Finger, R. (2014). Economic and environmental assessment of irrigation water policies: A bioeconomic simulation study. *Environmental Modelling & Software*, 51, 112–122. <http://dx.doi.org/10.1016/j.envsoft.2013.09.011>, URL <https://www.sciencedirect.com/science/article/pii/S1364815213002028>.
- Lopez-Jimenez, J., Quijano, N., & Vande Wouwer, A. (2021). An agent-based crop model framework for heterogeneous soils. *Agronomy*, 11(1), 85.
- Lopez-Jimenez, J., Quijano, N., & Vande Wouwer, A. (2023). Agent-based sensor location strategy for smart irrigation of large crop fields. *Computers and Electronics in Agriculture*, 214, Article 108282.
- Lozoya, C., Mendoza, C., Aguilar, A., Román, A., & Castelló, R. (2016). Sensor-based model driven control strategy for precision irrigation. *Journal of Sensors*, 2016.
- Lozoya, C., Mendoza, C., Mejía, L., Quintana, J., Mendoza, G., Bustillos, M., et al. (2014). Model predictive control for closed-loop irrigation. *IFAC Proceedings Volumes*, 47(3), 4429–4434.
- Luo, R., Bourdais, R., van den Boom, T. J., & De Schutter, B. (2017). Multi-agent model predictive control based on resource allocation coordination for a class of hybrid systems with limited information sharing. *Engineering Applications of Artificial Intelligence*, 58, 123–133.
- Moyroud, N., & Portet, F. (2018). Introduction to QGIS. *QGIS and Generic Tools*, 1, 1–17.
- Qin, S. J., & Badgwell, T. A. (2003). A survey of industrial model predictive control technology. *Control Engineering Practice*, 11, 733–764.
- Qin, S., Badgwell, T., Allgöwer, F., & Zheng, A. (2000). Nonlinear model predictive control. *Progress in Systems and Control Theory*, 26, 369–392.
- Raković, S., & Levine, W. (2018). Handbook of model predictive control. In *Control engineering*, Springer International Publishing.
- Rossiter, J. (2003). Model-based predictive control: A practical approach. In *Control series*, CRC Press.
- Sheshadri, S., Dann, B., Hueser, T., & Scherberger, H. (2020). 3D reconstruction toolbox for behavior tracked with multiple cameras. *Journal of Open Source Software*, 5(45), 1849.
- Yu, Q., Cheng, H. H., Cheng, W. W., & Zhou, X. (2004). Ch OpenCV for interactive open architecture computer vision. *Advances in Engineering Software*, 35(8–9), 527–536.